Tailoring Surface Acidity of Metal Oxide for Better Polysulfide Entrapment in Li-S Batteries

*Xiwen Wang, Tao Gao, Xiulin Fan, Fudong Han, Yiqing Wu, Zhian Zhang, Jie Li, and Chunsheng Wang**

The polysulfide shuttle reaction has severely limited practical applications of Li-S batteries. Recently, functional materials that can chemically adsorb polysulfide show significant enhancement in cycling stability and Coulombic efficiency. However, the mechanism of the chemisorption and the control factors governing the chemisorption are still not fully understood. Here, it is demonstrated for the first time that the surface acidity of the host material plays a crucial role in the chemisorption of polysulfide. By tailoring the surface acidity of TiO_2 via heteroatom doping, the polysulfide-TiO_2 interaction can be fortified and thus significantly the capacity fading be reduced to 0.04% per cycle. The discovery presented here sheds light on the mechanism of this interfacial phenomenon, and opens a new avenue that can lead to a practical sulfur/host composite cathode.

1. Introduction

Lithium-sulfur batteries (Li-S) have been regarded as the most promising alternative to conventional lithium-ion batteries (LIBs) due to its high energy density (2600 Wh Kg^{-1}).[1] Different from the intercalation mechanism of conventional LIB electrodes, the sulfur undertakes a conversion reaction pathway, in which S_8 is reduced to long-chain lithium polysulfide (PS), and further to lithium sulfide (Li_2S_2 and Li_2S).[2] The soluble long-chain PS (Li_2S_n, $n \geq 4$) tends to transport (both diffuse and migrate) into electrolyte during cycling, leading to the continual loss of active materials and inevitable redox shuttle effect.[3]

To address the issue, most efforts were devoted to physically trapping polysulfide within host structure. By impregnating sulfur into the pores of carbonaceous materials, sulfur utilization has been greatly enhanced due to sulfur's ready electron access and the extended interfacial reaction area.[4] However, physical confinement cannot completely eliminate loss of sulfur species during repeated cycles because the long tortuous pores and physical adsorption are not sufficient to retard the transport of PS into electrolyte under high concentration gradient and internal electric field. Introducing chemical interaction between functional groups/polar sites on the host with PS is emerging as a more effective approach for caging sulfur species.[5] Recent reports found that using functionalized carbon[6,7] and metal oxide[8] as sulfur host can significantly improve the cycling performance for Li-S cells. Density function theory calculation and surface chemistry analysis reveal that the polar–polar chemical interaction[9] between PS and the host are responsible for this performance improvement. In addition, the lone electron pairs of PS anion are prone to forming the strong Lewis acid–base bonds with the electron-accepting metal sites on host,[5] which have also been proven to capture PS and result in long-term cycling stability (89% after 100 cycles at 0.1 C) in latest report of metal-organic framework.[10] Nevertheless, the chemical nature of this interfacial phenomenon and the factors governing its strength are not well understood.

Herein, we systematically tuned the surface chemistry of a sample metal oxide host (TiO_2), investigated its interfacial interaction with PS, and demonstrated for the first time that the surface acidity of the host material plays a critical role in its capability to chemisorb PS. By tailoring the surface acidity of TiO_2 via heteroatom doping, we were able to enhance the polysulfide-TiO_2 interaction in the form of a strong Ti-S bond. Consequently, the doped TiO_2/S composite cathode exhibits significantly better capacity retention (0.040% fading per cycle) than pure TiO_2/sulfur composite (0.067% fading per cycle) and porous carbon/sulfur composite (0.114% fading per cycle). The discovery in our paper not only shed light on the mechanism of these unprecedented electrode-electrolyte interfacial phenomena, but also opens a new avenue for realizing practical Li-S battery with comparable capacity retention with intercalation cathode.

2. Results and Discussion

Assuming the chemisorption of PS on metal oxide originates from Lewis acid–base interaction (since PS anion tends to donate its lone electron pairs to the electron-accepting metal sites),[5,10] a host material with strong acidic surface should have better PS adsorption capability. To verify this hypothesis, we first intentionally fabricated metal oxide host with different

X. Wang, T. Gao, Dr. X. Fan, F. Han, Y. Wu, Prof. C. Wang
Department of Chemical and Biomolecular Engineering
University of Maryland
College Park, MD 20742, USA
E-mail: cswang@umd.edu
X. Wang, Prof. Z. Zhang, Prof. J. Li
School of Metallurgy and Environment
Central South University
Changsha 410083, China

DOI: 10.1002/adfm.201602264

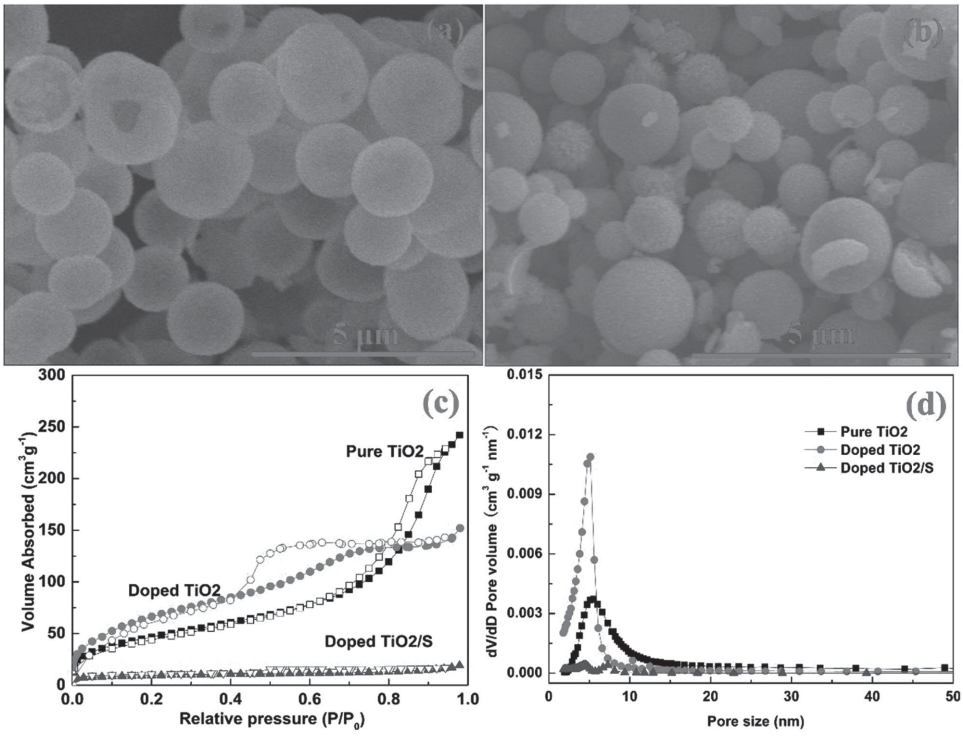

Figure 1. SEM images of a) doped TiO_2 and b) pure TiO_2. The hollow structure is confirmed by some broken outer shells and holes on spheres. c) N_2 absorption–desorption isotherms and d) pore size distribution of pure TiO_2, doped TiO_2, and doped TiO_2/S. (solid dots: adsorption branch, hollow dots: desorption branch).

surface acidity. We choose TiO_2 hollow nanosphere as a model sulfur host to demonstrate the concept because: (1) TiO_2 has been regarded as one promising host due to its high PS adsorption ability;[11] (2) the hollow nanosphere provides sufficient void space for high sulfur loading, volume expansion accommodation, and physical suppression of outbound PS transport.[12] B, N surface doping on TiO_2 was conducted through a one-step aerosol spray pyrolysis technique to tune the surface acidity of TiO_2.[13,14] Two types of TiO_2 (pure TiO_2 and doped TiO_2) share the similar morphologies of spherical shape with specific surface area of 168 ± 7 m^2 g^{-1} and pore volume of 0.35 ± 0.02 cm^3 g^{-1} (**Figure 1**).

B, N surface doping on TiO_2 was proved by X-ray photo-electron spectroscopy (XPS) results (Figure S1, Supporting Information). The chemical composition of B, N-doped TiO_2 should be Ti—O—Ti, Ti—N—O-Ti, Ti—B—O—Ti, and Ti—B—N—O—Ti linkage, in which B and N mainly occupy the interstitial sites in TiO_2 lattice (Figure S1b–d), which does not stimulate formation of Ti^{3+} species.[13] The Ti 2p peaks in doped TiO_2 show a noticeable increase of 0.5 eV in binding energy (**Figure 2**a), indicating an enhanced surface acidity of doped TiO_2.[14] NH_3 -temperature programmed desorption (TPD) measurements (Figure 2b), widely used in photocatalyst for evaluating the surface acidity of catalyst,[15] show evidently large amount of NH_3 is desorbed for doped TiO_2, in contrast to a small desorption peak in pure TiO_2, which further confirms the increase in surface acidity of doped TiO_2: In addition, the doped TiO_2 shows peaks for both weak and medium acid sites, while pure TiO_2 only has a peak for weak acid sites.

The effect of acidity of the TiO_2 on chemisorption of long-chain PSs was evaluated by electrochemical behavior of Ti_2O/S cathodes in Li-Ti_2O/S cell. Sulfur was impregnated into doped-TiO_2 matrix by a vapor phase infusion method[16] and a uniform distribution of sulfur can be observed (Figure S2, Supporting Information). The sulfur content of doped-TiO_2/S and pure TiO_2/S composites is measured to be 68 and 69 wt%, respectively (Figure S3, Supporting Information). Because of the relative low pore volume of both mesoporous TiO_2 host and high sulfur loading in corresponding sulfur composites, the slightly different pore size distribution (Figure 1d) of two TiO_2 has no effect on electrochemical performance of cathode, which excludes the influence of their physical properties and enables a fair comparison for their chemisorption effect.[17] The charge–discharge profiles of doped TiO_2/S (**Figure 3**a) and pure TiO_2/S (Figure 3b) cathode at 0.5 C in different cycles exhibit the typical pattern of Li-S batteries. The cycling stability of pure Ti_2O/S and doped Ti_2O/S is shown in Figure 3c and compared to the prevailing porous carbon-sulfur composite with a similar sulfur loading. The doped TiO_2/S, pure TiO_2/S, and porous carbon/S cathode present resembling initial discharge capacity of 1171, 1092, and 946 mAh g^{-1}, respectively. However, the doped TiO_2/S cathode demonstrates an exceptionally low capacity fading (0.04% per cycle), whereas the pure TiO_2/S cathode shows a higher value (0.067% per cycle) and the nonpolar porous carbon suffers much faster capacity fading (0.067% per cycle). Doped TiO_2 shows one of the best performances among all reported polar sulfur hosts, including MXene-Ti_2C,[18] Ti_4O_7,[19] H_2-reduced TiO_2,[20] and CTAB-graphene oxide.[21]

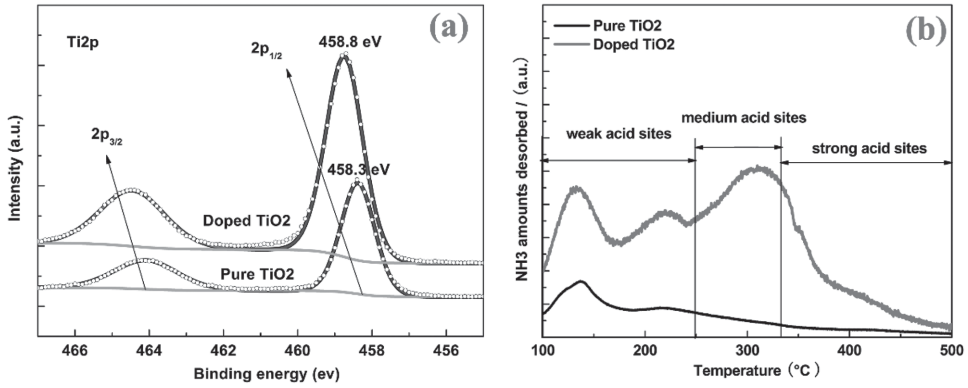

Figure 2. a) Ti 2p XPS spectra of doped TiO_2 and pure TiO_2. (round dots: experimental data; solid line: fitting results). b) NH_3 -TPD profiles of doped TiO_2 and pure TiO_2. The NH_3 desorption in temperature range of 100–250, 250–330, and 330–500 °C is generally ascribed to chemisorption of NH_3 by weak, medium, and strong acid sites, respectively.[15]

Apart from the long-term cycling tests, doped TiO_2/S and pure TiO_2/S cathodes were also cycled at different current densities. As shown in Figure S4 (Supporting Information), the discharge capacity of doped TiO_2/S cathode decreases more slowly than pure TiO_2/S cathode as the rates gradually increase from 0.2 to 6 C. It is important to note that a capacity of 424 mAh g^{-1} can be obtained at high rate of 6 C, indicating better kinetics of doped TiO_2/S cathode. The electrochemical impendence spectra are in good agreement with rate performance of these cathodes (Figure S5, Supporting Information). Doped TiO_2/S cathode has much lower interphase contact resistance and charge-transfer resistance than that of pure TiO_2/S cathode, which can be ascribed to the spatially controlled precipitation of sulfides on it, benefiting from the enhanced interaction of the PS with doped TiO_2.[19,22] Moreover, this enhanced interaction further renders the absence of self-discharge in cells with doped TiO_2/S cathode (Figure S6, Supporting Information). After rest for 3 d at the fresh state and the immediate state with maximal PS concentration (discharged to 2.1 V), the constant open-circuit voltage, and the discharge capacity were even slightly increased compared to the previous cycle, proving the firm PS stabilization by doped TiO_2/S host.[23,24]

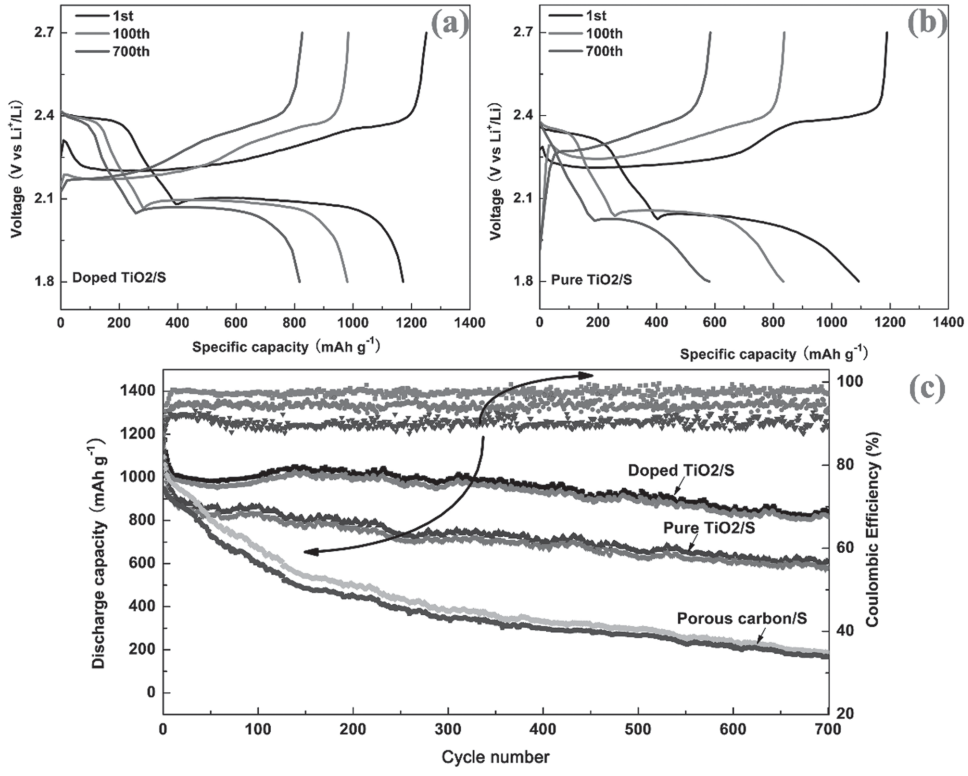

Figure 3. Galvanostatic voltage profiles of a) doped TiO_2/S and b) pure TiO_2/S cathode in different cycles at 0.5 C. c) Cycling performance and Coulombic efficiency of doped TiO_2/S, pure TiO_2/S, and porous carbon/S cathode at 0.5 C.

This significant improvement in capacity retention and self-discharge elimination with the doped TiO_2/sulfur cathode suggests a much stronger chemical interaction between TiO_2 and PS. To examine its strength, we mimic the chemisorption of PS in Li-S batteries by immersing the host materials into PS solutions (Li_2S_n in DOL/DME, $4 \le n \le 6$). The exceptional absorption capability of doped-TiO_2 to PS is confirmed by color difference recorded using digital photographs (**Figure 4**a). After 12 h

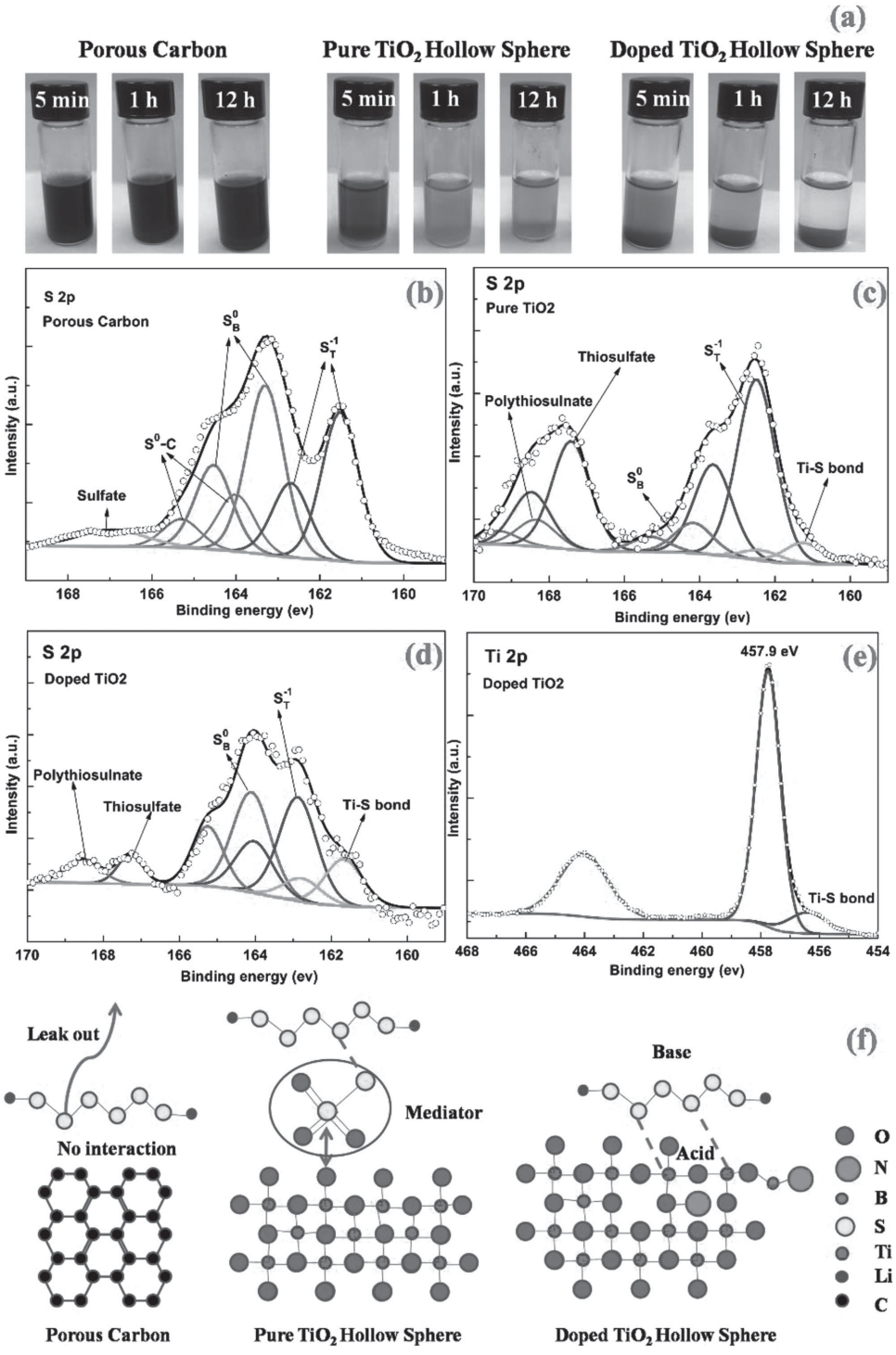

Figure 4. a) Digital photographs of porous carbon, pure TiO_2, and doped TiO_2 statured in Li_2S_n (in DOL/DME, $4 \le n \le 6$) solution and then rest for 5 min, 1 h, and 12 h; High resolution XPS S2p spectra of b) Li_2S_n infiltrated porous carbon, c) Li_2S_n infiltrated TiO_2, and d) Li_2S_n infiltrated doped TiO_2, e) Ti2p spectra of Li_2S_n infiltrated doped TiO_2; f) Schematic representation of chemical interaction of porous carbon, pure TiO_2, and doped TiO_2 to polysulfide.

rest, PS solution with doped TiO_2 became almost transparent, while pure TiO_2 one shows only slight color fading but the porous carbon one shows no clear change. The residual sulfur content in the supernatant was measured via ICP-OES. A large portion of total sulfur remains in the solution with presence of porous carbon (87.6%) and pure TiO_2 (29%), while only 2.4% of sulfur left in the solution of doped TiO_2 (Table S1, Supporting Information).

The remarkable PS chemisorption capability of doped TiO_2 is consistent with its exceptional capacity retention in the corresponding Li-S battery (Figure 3). To understand the nature of this chemisorption, the surface chemistries of these sulfur hosts after the adsorption experiment were analyzed with XPS. The S2p peaks of Li_2S_n at 161.5 and 163.0 eV could be attributed to terminal sulfur (S_T^{-1}) and bridging sulfur (S_B^0) respectively (Figure S5, Supporting Information).[19,25] For porous carbon, both S_T^{-1} and S_B^0 peaks show no change in the binding energy, and the peak at 163.8 eV for C-S^0 bonding was attributed to interaction between carbon and elemental S^0 generated from Li_2S_4 disproportion,[19] indicating no chemical interaction between porous carbon and PS (Figure 4b). By contrast, both S_T^{-1} and S_B^0 peaks of TiO_2 undergo a positive shift in binding energy, especially for doped TiO_2 (1.4 eV), resulting from the paring of Lewis acid sites on the surface of TiO_2 with PS (Figure 4c,d).[26] This Lewis acid–base interaction is more evidently seen by additional peaks that correspond to Ti-S bond at ≈161.5 eV in the S2p spectrum of both TiO_2[9,27] and at 456.5 eV in Ti 2p spectrum of the doped TiO_2.[9,28] Another set of peaks at 167.2 and 168.0 eV is indicative of thiosulfate and polythionate complex, which can bind PS through a mediation effect.[29] The mechanism of PS chemisorption is illustrated in Figure 4f. It is noteworthy that the doped TiO_2 shows more intense Ti-S bond peaks and less intense thiosulfate/polythionate peaks than pure TiO_2. Despite both Ti-S bond and thiosulfate/polythionate complex are responsible for the chemisorption of PS, the Ti-S bond plays a more substantial role in it, because the doped TiO_2 with a stronger Ti-S bond has better capacity retention and more rapid PS adsorption than pure TiO_2.

3. Conclusion

In summary, we have demonstrated that stronger surface acidity of metal oxide host enables much higher polysulfide chemisorption capability (97.6% sulfur species after 12 h), and thus remarkably better cycling performance for Li-S batteries (0.04% capacity fading per cycle). This strengthened polysulfide chemisorption can be well explained by Lewis acid–base theory, based upon which the surface acidity enhanced TiO_2 host forms a stronger Ti-S bond with the Lewis basic PS anion than pure TiO_2 and porous carbon, thus better PS chemisorption. This systematic study not only provides direct chemical evidence for the previously reported Lewis base–acid interaction in Li-S batteries, but also identifies the governing factor for PS chemisorption capability, which opens a new pathway for realizing practical Li-S battery. More broadly, the chemical insights regarding these unprecedented interfacial phenomena in Li-S batteries may have a profound influence on the community's understanding of other multiphase electrochemical energy systems including flow battery, iodine battery, etc.

4. Experimental Section

Materials Preparation: All chemicals were purchased from Sigma-Aldrich and used as received. The B, N-doped TiO_2 hollow nanospheres were fabricated through a spray pyrolysis method using the spray pyrolysis reactor system. 10 mmol boric acid and 10 mmol urea were dissolved in 100 mL distilled water, and then 10 mmol $TiCl_4$ was slowly added into the solution above in the ice bath. The precursor solution was nebulized via ultrasonic droplet generator (1.7 MHz), thereby creating the fine aerosol droplets. Then these droplets were carried by nitrogen gas at flow rate of 3 L min^{-1} into quartz reaction tube and were maintained at 600 °C. The particles were collected on a PTFE filter using a brush, washed and finally dried in oven at 60 °C.

To synthesize B, N-doped TiO_2/S composites, sublimed sulfur and B, N-doped hollow nanospheres were mixed in a weight ratio of 3:1 and sealed in a glass tube under vacuum condition. This sealed tube was annealed in an oven at 600 °C for 3 h with heating ramp of 5 °C min^{-1}. After cooling down to room temperature, the powder was collected. For comparisons, pure TiO_2 nanospheres prepared by solvothermal method using 1, 2-propanediol[30] and porous carbon (ACS Material LLC, USA) were used as sulfur host. The corresponding sulfur-based composites were prepared by the same vapor phase infusion process as above.

Material Characterizations: The surface morphology of samples was investigated by scanning electron microscope (SEM, Hitachi Su-70, Japan). BET surface area, pore size, and volume were tested using N_2 adsorption/desorption measurement on Micromeritics ASAP 2020 (Micromeritics Instrument Crop., USA). Samples were degassed at 100 °C under vacuum for 12 h before the test. The specific surface area was calculated from the nitrogen adsorption branch using the BET method. The porosity distribution was calculated from the adsorption branch using the Barrett–Joyner–Halenda method. Surface chemistry of samples was examined via X-ray photoelectron spectroscopy (XPS, Kratos Axis 165, USA) using monochromatic Al Kα radiation at room temperature. All reported binding energy values were calibrated to the C 1s peak at 284.8 eV. Peak fitting was done using CASA XPS software. Data were fit with a Shirley background using peaks with a 30% Lorentzian, 70% Gaussian product function. S 2p spectra were fit with spin-orbit split 2p3/2 and 2p1/2 doublets, constrained by 1.18 eV separation and a characteristic 2:1 area ratio. All peaks were constrained to have the same FWHM. The acidity of samples mined by ammonia (NH_3) temperature programmed desorption (TPD) with a mass spectrometer (MS, Ametek Proline). Prior to measurement, 0.1 g of sample was loaded in a U shape quartz tube and activated by heating in a He (30 mL min^{-1}, Airgas) flow at 600 °C for 3 h. After cooling to 100 °C, NH_3 adsorption was carried out. Physically adsorbed NH_3 was removed by a He flow (60 mL s^{-1}) at 100 °C for 2 h. The NH_3-TPD of the samples was carried out by increasing the temperature linearly from 100 to 500 °C with a heating rate of 10 °C min^{-1}. Thermogravimetric (TG, SDTQ600) analysis was conducted in determining the sulfur content in the composites under an argon atmosphere.

Electrochemical Measurements: The sulfur-based active materials were manually mixed with acetylene black and sodium alginate binder in weight ratio of 80:10:10, with suitable amount of distilled water to form slurry. Then, the slurry was uniformly cast onto the carbon paper (Toray, TGP-H-120) by a doctor blade and dried in vacuum oven at 60 °C overnight. The typical mass loading of active materials on each electrode was 1.3~1.5 mg cm^{-2}. All electrochemical studies were performed using 2025 coin cells which consist of a lithium metal anode, a Celgard 3501 separator and a cathode. The cells were assembled in an argon-filled glove box and 1 M bis(trifluoromethane) sulfonamide lithium salt (LiTFSI, Sigma Aldrich) in a mixture of 1,3-dioxolane (DOL) and 1,2-dimethoxyethane (DME) (v/v, 1:1) with 1 wt% $LiNO_3$ was used as the electrolyte. The voltage window of galvanostatic test was estimated

in the range from 1.8 to 2.7 V in consideration to prevent TiO_2 lithiation and Ti^{4+}/Ti^{3+}[20] transition. Both the specific capacities and current densities were calculated on the basis of the mass of sulfur.

Supporting Information

Supporting Information is available from the Wiley Online Library or from the author.

Acknowledgements

The authors thank Dr. Karen J. Gaskell at the Surface Analysis Center of University of Maryland for the help with the XPS test and data analysis, Prof. Dongxia Liu at the Department of Chemical and Biomolecular Engineering of University of Maryland for the help with NH_3–TBD measurements. X.W.'s fellowship was supported by China Scholarship Council (Grant No. 201406370037). This work was also supported by Nanostructures for Electrical Energy Storage (NEES), an Energy Frontier Research Center funded by the U.S. Department of Energy, Office of Science, Office of Basic Energy Sciences under Award No. DESC0001160.

Received: May 7, 2016
Revised: July 2, 2016
Published online: August 3, 2016

[1] A. Manthiram, Y. Fu, S. Chung, C. Zu, Y. Su, *Chem. Rev.* **2014**, *114*, 11751.
[2] C. Barchasz, F. Molton, C. Duboc, *Anal. Chem.* **2012**, *84*, 3973.
[3] Y. V. Mikhaylik, J. R. Akridge, *J. Electrochem. Soc.* **2004**, *151*, A1969.
[4] X. Ji, K. T. Lee, L. F. Nazar, *Nat. Mater.* **2009**, *8*, 500.
[5] Q. Pang, X. Liang, C. Y. Kwok, L. F. Nazar, *J. Electrochem. Soc.* **2015**, *162*, A2567.
[6] J. Song, T. Xu, M. L. Gordin, P. Zhu, D. Lv, Y. B. Jiang, Y. Chen, Y. Duan, D. Wang, *Adv. Funct. Mater.* **2014**, *24*, 1243.
[7] S. Yuan, J. L. Bao, L. Wang, Y. Xia, D. G. Truhlar, Y. Wang, *Adv. Energy Mater.* **2016**, *6*, 1501733.
[8] W. Li, J. Hicks-Garner, J. Wang, J. Liu, A. F. Gross, E. Sherman, J. Graetz, J. J. Vajo, P. Liu, *Chem. Mater.* **2014**, *26*, 3404.
[9] X. Tao, J. Wang, Z. Ying, Q. Cai, G. Zheng, Y. Gan, H. Huang, Y. Xia, C. Liang, W. Zhang, Y. Cui, *Nano Lett.* **2014**, *14*, 5288.
[10] J. Zheng, J. Tian, D. Wu, M. Gu, W. Xu, C. Wang, F. Gao, M. H. Engelhard, J. G. Zhang, J. Liu, J. Xiao, *Nano Lett.* **2014**, *14*, 2345.
[11] Z. Wei Seh, W. Li, J. J. Cha, G. Zheng, Y. Yang, M. T. McDowell, P.-C. Hsu, Y. Cui, *Nat. Commun.* **2013**, *4*, 1331.
[12] N. Jayaprakash, J. Shen, S. S. Moganty, A. Corona, L. A. Archer, *Angew. Chem. Int. Ed.* **2011**, *50*, 5904.
[13] N. Feng, A. Zheng, Q. Wang, P. Ren, X. Gao, S. Bin Liu, Z. Shen, T. Chen, F. Deng, *J. Phys. Chem. C* **2011**, *115*, 2709.
[14] Y. Su, S. Han, X. Zhang, X. Chen, L. Lei, *Mater. Chem. Phys.* **2008**, *110*, 239.
[15] B. Naik, K. M. Parida, C. S. Gopinath, *J. Phys. Chem. C* **2010**, *114*, 19473.
[16] J. Guo, Y. Xu, C. Wang, *Nano Lett.* **2011**, *11*, 4288.
[17] X. Li, Y. Cao, W. Qi, L. V. Saraf, J. Xiao, Z. Nie, J. Mietek, J.-G. Zhang, B. Schwenzer, J. Liu, *J. Mater. Chem.* **2011**, *21*, 16603.
[18] X. Liang, A. Garsuch, L. F. Nazar, *Angew. Chem. Int. Ed.* **2015**, *54*, 3907.
[19] Q. Pang, D. Kundu, M. Cuisinier, L. F. Nazar, *Nat. Commun.* **2014**, *5*, 4759.
[20] Z. Liang, G. Zheng, W. Li, Z. W. Seh, H. Yao, K. Yan, D. Kong, Y. Cui, *ACS Nano* **2014**, *8*, 5249.
[21] M. Song, Y. Zhang, E. J. Cairns, *Nano Lett.* **2013**, *13*, 5891.
[22] Z. Deng, Z. Zhang, Y. Lai, J. Liu, J. Li, Y. Liu, *J. Electrochem. Soc.* **2013**, *160*, A553.
[23] Y. Xu, Y. Wen, Y. Zhu, K. Gaskell, K. A. Cychosz, B. Eichhorn, K. Xu, C. Wang, *Adv. Funct. Mater.* **2015**, *25*, 4312.
[24] C. J. Hart, M. Cuisinier, X. Liang, D. Kundu, A. Garsuch, L. F. Nazar, *Chem. Commun.* **2015**, *51*, 2308.
[25] I. J. Kartio, C. I. Basilio, R. Yoon, *Langmuir* **1998**, *14*, 5274.
[26] H. Metiu, S. Chretien, Z. Hu, B. Li, X. Sun, *J. Phys. Chem. C* **2012**, *116*, 10439.
[27] G. Xu, J. Yuan, X. Tao, B. Ding, H. Dou, X. Yan, Y. Xiao, X. Zhang, *Nano Res.* **2015**, *8*, 3066.
[28] H. Martinez, C. Auriel, D. Gonbeau, M. Loudet, G. Pfister-Guillouzo, *Appl. Surf. Sci.* **1996**, *93*, 231.
[29] X. Liang, C. Hart, Q. Pang, A. Garsuch, T. Weiss, L. F. Nazar, *Nat. Commun.* **2015**, *6*, 5682.
[30] Y. Zhao, Q. Chen, F. Pan, H. Li, G. Q. Xu, W. Chen, *Chem. Eur. J.* **2014**, *20*, 1400120.